Synthesis, characterization and mechanical properties of $(Al, Cu)_3Ti$ powder blend by mechanical alloying

A thesis submitted in partial fulfillment of the
requirements for the degree of

Master of Technology
in
Metallurgical and Materials Engineering

by

Sitikantha Behera
Roll No. 212MM1447

Department of Metallurgical and Materials Engineering
National Institute of Technology Rourkela
Rourkela, Orissa-769008

Synthesis, characterization and mechanical properties of $(Al, Cu)_3Ti$ powder blend by mechanical alloying

A thesis submitted in partial fulfillment of the
requirements for the degree of

Master of Technology
in
Metallurgical and Materials Engineering

by
Sitikantha Behera
Roll No. 212MM1447

Under the guidance
of
Prof.(Dr.)D.Chaira

Department of Metallurgical and Materials Engineering
National Institute of Technology Rourkela
Rourkela, Orissa-769008

National Institute of Technology
Rourkela

Declaration

I endorse that

a) The work contained in the dissertation is original and has been managed by myself under the general superintendence of my supervisor.

b) The study has not been acceded to any other university for any grade or degree.

c) I have adopted the guidelines offered by the Institute in writing the dissertation.

c) Whenever I have used materials (experimental analysis, and text) from other informants, I have given due acknowledgment to them by mentioning them in the textbook of the thesis and giving their details in the references.

e) Whenever I have quoted written materials from other informants, I have put them under quotation marks and given due acknowledgment to the sources by citing them.

Date: **Sitikantha Behera**

National Institute of Technology
Rourkela

Certificate

This is to certify that the dissertation entitled **"Synthesis, characterization and mechanical properties of $(Al, Cu)_3Ti$ powder blend by mechanical alloying** " submitted by Sitikantha Behera (212MM1447) in the fulfilment of the prerequisites for the award of Master of Technology in Metallurgical and Materials Engineering at the National Institute of Technology, Rourkela is a benefice research work carried out by him under my supervision and direction.

To the best of my knowledge, the matter embodied in the thesis is based on candidate's own work has not been submitted to any other university institute for the laurels of any degree or diploma.

Date:

Supervisor

Prof.(Dr.) D. Chaira

Metallurgical and materials engineering

National Institute of Technology

Rourkela-769008

Acknowledgement

I take immense pleasure in thanking and wish to express my deep sense of gratitude to my project guide **Prof.D.Chaira, Department of Metallurgical and Materials Engineering, NIT Rourkela** for his able guidance and useful suggestions. It would not been possible for me to bring out this report without his assistance and encouragement.

I convey my sincere gratefulness to **Prof.B.C.Ray**, Head of the Department, Metallurgical and Materials Engineering, NIT Rourkela for giving me an opportunity to go on this task and granting me the access to valuable facilities in the department.

My particular thanks go to **Prof.S.KSahoo**, **Prof.S.C.Mishra**, **Prof.S.K.Karak** for providing facility and giving me the valuable suggestion to carry out this project and also all professors of this department. I am extremely grateful to laboratory members of the Department of Metallurgical and Materials Engineering, N.I.T., Rourkela, especially, Mr.U.K.Sahu, Mr. Pradhan, Mr.A.Pal, Mr.Shyamu Hembram, Mr.Rajesh Pattnaik and Mr.Kishore Tanty for their assistance during the carrying out of experiments.

Last but not the least I would like to thank, Shashanka , Pankajini Sahani and Mohan, all my classmates and my dear friends Jaykishan Dora, Kishore Ku Mahato, Bibhudutta Bishoyi, Sumant Samal ,Deepak Ku Bhunya, Abhilash Purohit, George Lenin and Jay kumar for their encouragement and sympathy. Most importantly, none of this would have been possible without the love and patience of my family.

Sitikantha Behera

Abstract

In the present investigation, an attempt has been made to study the formation of intermetallic compound for $Al_{70}Cu_{22}Ti_8$ alloy composition by mechanical alloying. Elemental powder of $Al_{70}Cu_{22}Ti_8$ (all in wt. %) composition was milled in a Fritsch pulverisette planetary mill for 50h under toluene. Powder of 1wt. % Y_2O_3 and 1wt. % TiO_2 were added separately to the 50 h milled base alloy powder to study the effect of oxide dispersion. X-Ray diffraction shows the formation of AlCu, $AlTi_3$, and Cu_9Al_4 intermetallics compound formation after 50h of milling. There is a formation of Al_2O_3 for Y_2O_3 and TiO_2 dispersed base alloy sintered at all temperatures. It has been observed that the rate of reduction of size is very fast up to 10h of milling and after that it is gradually decreases and remains constant after 10 h of milling. Particle size has been reduced from 45 μm to 6 μm after 50 hour of milling. DSC study shows the presence of small endothermic peak at 535^0C for formation of Al_2Cu and two exothermic peaks at 701^0C and 850^0C for formation of other intermetallics like $AlTi_3$, Cu_9Al_4 and AlCu. A maximum of 81% theoretical density was obtained for the composite powder mixture sintered at 1100^0C for 1h. A maximum Vickers microhardness of 449, 649, 872HV were obtained for base alloy, Y_2O_3 and TiO_2 dispersed alloy sintered at 1100^0C for 1h respectively. It was also found that TiO_2 and Y_2O_3 dispersed base alloy have higher wear resistance than base alloy.

Contents

Page No:

List of Figures

List of Tables

Chapter 1

Introduction

This chapter describes the importance and applications of intermetallics and Al_3Ti intermetallics. In this chapter, objectives of the project are also presented.

1 Introduction

1.1 Background

In earth crust aluminium is present in hydrated oxide form of which bauxite is the primary ore. The aluminium alloys are light weight ($2.77g/m^3$) and easy to manufacture. Aluminium alloys have high specific strength approximately 3 times that of structural steel. So, aluminium alloys are primary used for consumption and production after steel [1].

But today's modern world calls for materials with a combination of properties that cannot be met by single metal like polymer, ceramic and metal alloys. This combination of material properties is achieved by the development of intermetallic [2].

Intermetallic is new class of most advanced materials. Intermetallic have different crystal structure than that of the parent materials. The intermetallic compound formation occurs when the bond strength of similar atoms (Al-Al) is less than that of bond strength of unlike atoms (Al-Ti). Intermetallic have properties between metal and ceramics because they have order distribution of atom [3].

Intermetallics have high structural material because they have high oxidation resistance, low density and high melting point temperature etc [4-9]. Intermetallic can replace the super alloy and stainless steel as they process high melting point [10]. Intermetallic widely applied for high temperature structural application so they generally used in jet engine to withstand the operating temperature and reduce the weight of the engine.

At room temperature most of intermetallics have less toughness and the manufacturing cost of intermetallic compound is too high. Due to extrinsic factor the ductility of intermetallic is less but exception is FeAl intermetallic.

Al_3Ti intermetallic has low density i.e. 3.31g/cm^3 and high oxidation resistance [11]. At room temperature the Al_3Ti intermetallic shows 216 GPA of young's modulus which is more than other titanium aluminaides. Most super alloys have this range of young's modulus hence it can substitute super alloy. As Al_3Ti intermetallic is light weight it is used in aerospace application [12]. At low temperature Al_3Ti intermetallic is brittle but when exposed to air Al_2O_3 layer formation occurs as a result oxidation resistance increases [10, 11].

Al_3Ti intermetallic is order body centre tetragonal structure. So Al_3Ti intermetallic has less number of slip system .Hence it is less ductility .To improve the ductility of Al_3Ti intermetallic there are two steps [13].

i. Micro alloying of order body centre tetragonal structure [14].
ii. By adding the fourth period element of Cr, Fe, Ni, Cu, Zn etc. When it is added to Al_3Ti intermetallic the BCT structure changes to SC structure [15, 16, 17].

Intermetallics used in industrial applications are-

i. Titanium aluminides is used for aerospace application.
ii. Nickel aluminides is used for gas turbine application.
iii. Some of the automobile components are made of iron aluminides.

1.2 Objective of Project

The primary aims of the present investigation are

1. Preparation of aluminium based (Al, Ti and Cu) intermetallic compounds by planetary milling.
2. Characterization of milled intermetallic powder by various characterization techniques and subsequent consolidation by conventional sintering.
3. Study of mechanical property and physical properties of Al based intermetallic
4. Study of thermal conductivity of Al based intermetallic.
5. Study of wear resistance of Al based intermetallic.

1.3 Scope of project

This thesis includes seven chapters. First chapter explains the background of intermetallic, properties and applications. A brief description of mechanical alloying and literature review are presented in second chapter. Third chapter elaborates the detailed experimental parameters and procedure adopted. Results and discussions are briefly enumerated in chapter four. Conclusion or overall finding of experiments is described in chapter five. Chapter six and seven present the future scope of our work and references.

Chapter 2
Literature review

This chapter includes the literature review and available research work on Al_3Ti based intermetallics.

2. Literature review

2.1 Introduction

Aluminium alloy has several severe properties like low weight because of minimum density, high strength to weight ratio and good conductor of electricity so it is also widely used in several areas like construction, automobile, aerospace etc. Aluminium alloy of the 4×××, 5××× and 6××× series, containing major element additives of Mg and Si, are now being used to replace steel plants of various automobile industries [1, 18].

But today's modern world calls for materials with a combination of properties that cannot be met by single metal like polymer, ceramic and metal alloys. This combination of material properties is achieved by the development of intermetallic [1, 2]. Intermetallic is a new class of most advanced material. Intermetallic compounds and phases form due to combination of various metals. The crystal structure of the intermetallic compounds is different from those parent metals. The intermetallic compound formation occurs when the bond strength of similar atoms (Al-Al) is less than that of bond strength of unlike atoms (Al-Ti). Primary bond between the intermetallic is metallic bonding but not all intermetallic have this bond [3].

Phase transition occurs from the ordering reaction in the solid solution lattice of parent elements at a transition temperature from which a super lattice structure can create [3].

Example- Phases of Fe_3Al forms by ordering from the BCC solid solution from given bellow figure 2.1.

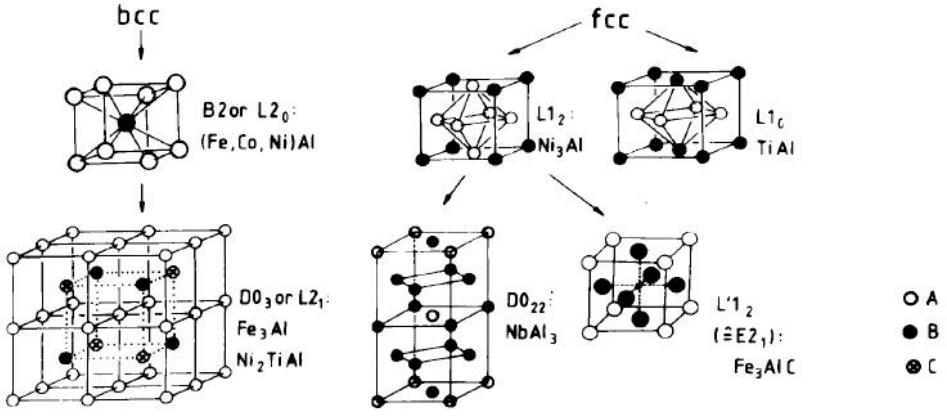

Figure 2.1 Intermetallics derived from BCC and FCC structures respectively [3]

Table 1 Some of the applications of intermetallics [3].

Intermetallics	**Phase**	**Applications**
cementation	Cu_3As	Coating of bronze tool
Yellow brass	CuZn	Coins, Ornamental parts
Amalgam	$Ag_2 Hg_3 + Sn_6Hg$	Dental restore
High tin bronze	$Cu_{31}Sn_8$	Mirror
Type metal	SbSn	printing
Acutal	$(Cu, Mn)_3Al$	Fruit knife
permalloy	Ni_3Fe	High permeability magnetic alloy
permendur	FeCo(-2V)	Soft magnetic alloy
Alnico	NiAl-Fe-Co	Permanent magnet material
sendust	$Fe_3(Si, Al)$	Magnetic head material
Cu-Al-Ni	$(Cu, Ni)_3Al$	Shape memory alloy
Aluminide coating	NiAl, CoAl	Surface coating for protection from environment
Kanthal super mosilit	$MoSi_2$	Electric heating elements
A 15 Compound	Nb_3Sn	Super conductors
Nitinol	NiTi	Shape memory alloy
Co-Sm magnet	Co_5Sm	Permant magnets

A number of modern techniques are being used to synthesize of nanostructured materials including

(1) Inert gas condensation
(2) Rapid solidification
(3) Electro deposition
(4) Sputtering
(5) Chemical processing
(6) Mechanical alloying

2.2 Mechanical Alloying

Mechanical alloying (MA) is defined as high-energy ball milling process. In MA two or more elemental powders are blended, cold welded and fragmented repeatedly and produces uniform powder mixture. In MA stable or metastable phase with finer microstructure are produced [19, 20, 21].

Mechanical alloying was first produced by John Benjamin et al. at International Nickel company in the year 1960's instead of produce oxide dispersion strengthened (ODS) alloys for high temperature applications [21].

MA coined as non equilibrium method for processing in the year 1980. Now a days MA is used to synthesize stable and metastable crystalline phases, nano crystalline material, intermetallic compound, quasi crystals and non equilibrium structures [20, 21].

Historical development of mechanical alloying

- 1966 Development of ODS nickel-base alloys
- 1981 Amorphization of intermetallic
- 1982 Disordering of ordered compounds
- 1983 Amorphization of blended elemental powder mixtures
- 1988 Synthesis of nanocrystalline phases
- 1989 Mechanochemical synthesis
- 1989 Synthesis of quasicrystalline phases
- 1991 Synthesis of high pressure polymers

2.2.1 Component of Mechanical alloying

i. Raw material

ii. Process variable

Raw material

In MA, generally, particle sizes of 1-200μm size of raw material are used. In order to produce novel material normally the power mixture of ductile-ductile, ductile-brittle and brittle-brittle powders are used in MA.

Later on a few minutes of milling of particle size decreases exponentially with respect to time and the powder particles becomes very small in micron. So, powder particle size is not really decisive, except that it should be smaller than the grinding ball size. Mostly the raw powders are refractory compound and pure elemental metals. Dispersion strengthening materials normally contain additions of carbides, nitrides, and oxides and they are known as oxide-dispersion strengthened (ODS) materials. Oxide dispersion improves mechanical properties [20].

Process Variable

Mechanical alloying is a complex procedure and therefore requires an optimal value of different variables to achieve the desired product phase. Some of the milling parameters that affect the final composition of the powder are:

- Type of mill
- Milling container
- Milling speed
- Milling time
- Type, size, and size distribution of the grinding medium
- Ball-to-powder weight ratio
- Extent of filling the vial
- Milling atmosphere
- Process control agent
- Temperature of milling

2.2.2 Mechanism of Mechanical alloying

In planetary mill, centrifugal force is generated due to rotation of the vials. Inside the vials grinding balls is present. Direction of vials and supporting disk is opposite to each other so centrifugal force inside the vials plays important role to move the ball. Particles were trapped by grinding ball after each collision. The impact force breaks the particle and creates a new clean surface. The new clean surfaces may be oxidised; generally MA is carried by inert gas or toluene. The collision against the opposite inside the wall gives the required impact force. Approximately around 1000 and 1500 particles are formed in each collision [20, 21]

Higher compressive strength given to grinding medium during milling for facilitating of inter particle welding. Normally the presence of malleable constituent act as binder for some other element. The smaller particles weld together and forms larger size. Then they became harder as a result the loose deformation characteristic. The ball strikes it again and breaks in to very small pieces. After some time of alloying, the particle size becomes constant [21].

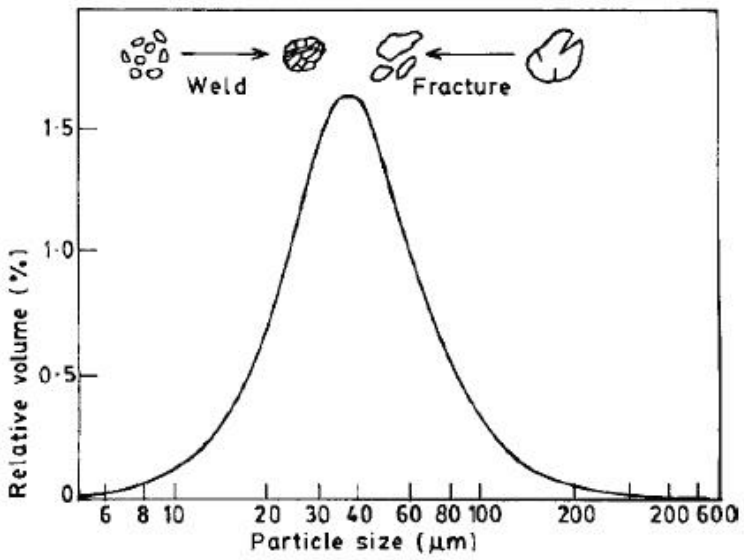

Figure 2.2 Balance between welding and fracturing [21]

2.2.3 Benefit of Mechanical Alloying

The MA process has several advantages:

1. The fine powders are homogeneous, which does not depend of the initial powder size.
2. Fine homogeneous dispersions can be held in a particle size of 1μm or less of a high concentration of alloying elements without blocking air.
3. Grinding times are reduced to 1/10th or even less than the time required in a conventional ball mill.
4. In mechanical alloying extremely fine dispersion of one of the metals in the other can be achieved, if the two metals are insoluble in solid state or in liquid state.
5. In other respect Mechanical alloying is a cold alloying process. Mechanical alloying has been applied for developing alloys from immiscible solids, intermetallics and metastable phases.

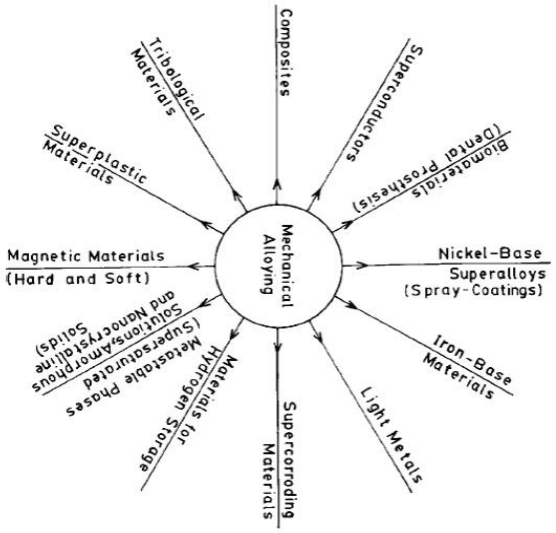

Figure 2.3 Application area of mechanical alloying [21]

2.2.4 Problem of Mechanical Alloying

Preparing and processing of nanoparticles by MA is the nature and amount of impurities that contaminate the milled powder. Contamination can arise from several sources

- Impurities in starting powders
- Vials and grinding media
- If the powders is added to the control agents.

2.3 Sintering

In powder metallurgy technique, one of the important steps is consolidation or sintering of green compact. Sintering defined as the process of firing and consolidation of powder at temperature less than equal to half of melting temperature. Here mass transfer occurs by diffusion process and the formation of a compact body occurs [22]. The various sintering mechanisms are:

1. Surface diffusion
2. Vapour transport
3. Lattice diffusion from surface
4. Lattice diffusion from grain boundary
5. Grain boundary diffusion
6. Plastic deformation

During sintering, mass transport from one place to another place and two particles are joined together and form a neck. As sintering proceeds neck becomes large by void shrinkage and finally a dense product is formed.

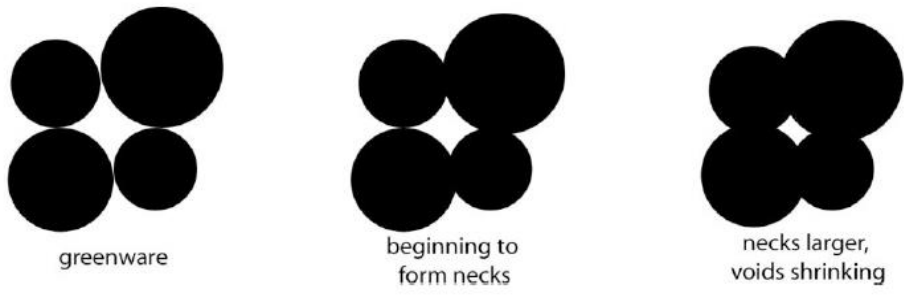

Figure 2.3 The formation of neck during sintering.

Srinivasan et al. studied the synthesis of $Al_{80}Ti_{20}$ and $Al_{90}Ti_{10}$ alloy by mechanical alloying followed by hot pressing. They found the compressive strength of $Al_{80}Ti_{20}$ and $Al_{90}Ti_{10}$ to be 1.25Gpa and 0.6Gpa respectively [23].

Watanabe et al studied the wear behaviour of Al-Al_3Ti composite and showed that wear resistance is more for the composite as compared to pure Al. The found that the supersaturated Al_3Ti layer formation occurs from the top surface to 100μm depth. On the surface supersaturated layer formation was occurred [24].

Milman et al studied the mechanical properties of Al_3Ti phase in $Al_{61}Cr_{12}Ti_{27}$ and $Al_{66}Mn_{11}Ti_{23}$ and determined the hot hardness at the temperature range 20^0C to 900^0C. The tetragonal Al_3Ti crystal structure was converting to cubic structure by adding of element Cr and Mn to form intermetallic and there is a decrease in hardness. The yield stress of these intermetallics of Al_3Ti, $Al_{61}Cr_{12}Ti_{27}$, and $Al_{66}Mn_{11}Ti_{23}$ decreases respectively [25].

Lee et al observed that pore-free bulk compacts and grain sizes of 8 to 10 nm are produced by using planetary ball milled of (Al 12.5 at.% Cu)$_3$Zr and (Al 12.5 at% Mn) powders. SPS-processed samples was measured to be 975.8 and 983.9 HV of micro-hardness respectively. They discovered that a grain refinement towards the nano scale does not induce an effect on improving fracture toughness in brittle intermetallic. By addition of boron and followed by annealing the fracture toughness increased [26].

Nayak et al observed that mechanical alloying of $Al_{75}Ti_{15}Zr_{10}$ base alloy is used to synthesis of Al_3(Ti,Zr) intermetallic. Alloying of the Al_3Ti intermetallic with Zr shows hardness decreases and Al_3Zr intermetallic with Ti shows plasticity decreases. If combined addition of Ti and Zr element to intermetallic alloys gave the result hardness decreases. Hardness of 2.43 GPa was showed by the Al_3Ti intermetallic. The addition Zr in to Al_3Ti hardness increases and 10% Zr containing intermetallic have maximum value is 3.23GPa and then value is fall for the $Al_{75}Zr_{25}$ composition (Al_3Zr) to be 2.57GPa [27].

Wang et al. investigated the $Al_{69}Ti_{25}La_6$ intermetallic and they found that fine and uniform particles were forming with increasing milling time. Vickers hardness (HV) was increased very fast at the initial stage of milling; increased very slowly at the later stages of milling. They also found that, Vickers hardness of Al-Ti and Al-Ti-La powders were decreased with increased annealing time but, it is higher for Al-Ti powders compared to the Al-Ti-La powders [28].

Fu et al observed the synthesis of $Al_{67}Mn_8Ti_{25}$ alloy by conventional casting process. Adding a small amount of Nb in the $Al_{67}Mn_8Ti_{25}$ alloy shows more strengthening and toughening effects. They found that powder consolidated sample is having higher fracture toughness than the cast sample [29].

Heilmaier et al studied synthesis of Al_3Ti by MA of elemental composition $Al_{67}Ti_{25}Cr_8$. They milled the powder of $Al_{67}Ti_{25}Cr_8$ composition and then hot pressing was conducted with addition of 3 vol. % Y_2O_3. They found that intermetallics with ODS have desired mechanical properties. They showed that equiaxed grains with nanometer range may improve low temperature ductility and toughness. Whereas, coarse and elongated grain structures improve the creep resistance at high temperatures [30].

Chapter 3
Experimental details

This chapter provides the experimental procedure followed for synthesis of intermetallics. Here, procedure of mechanical alloying and consolidation of mechanically alloyed powders has been discussed. A brief description of various characterization techniques like XRD, SEM, OM, FESEM, PSA are also presented. Experimental procedure for measurement of density, wear, micro hardness, wear volume and thermal conductivity are included here.

3 Experimental details

3.1 Synthesis of $(Al, Cu)_3Ti$ powder blend

Synthesis of $(Al, Cu)_3Ti$ powder blend were performed by mechanical alloying followed by conventional pressureless sintering.

Elemental powder of the composition $Al_{70}Cu_{22}Ti_8$ (all in wt. %) were milled for 0, 10, 20, 30, 40 and 50 h in a Fritsch pulverisette planetary mill. To avoid oxidation of powders during milling toluene ($C_6H_5CH_3$) was used to fill to just pass over the balls and powders. The details of milling parameters are mentioned in Table 2.

Fifty hours milled base powders were mixed separately with 1 wt. % of Y_2O_3 and TiO_2 powders by pestle and mortar for 1 hour. Then the mixed powders were cold compacted by hydraulic press using a load of 450MPa. Pellets of 15mm diameters were prepared by cold compaction. The cold compacted pellets were then sintered in a tubular furnace at 900°C, 1000°C and 1100°C for different times under a flowing argon gas. The different sintering parameters used are represented in Table 3.

Table 2 Milling parameters used for planetary milling of $(Al , Cu)_3Ti$

Milled parameter	**Value**
Rotation speed (rpm)	300
Ball-power weight ratio	5:1
Al: Cu: Ti (wt%)	70:22:8
Type of ball	steel
Milling time (h)	0 , 10 , 20 , 30 , 40 , 50
Grinding medium	toluene
Cointainer volume (ml)	250
Steel ball size (mm)	15 , 10

Table 3 Sintering parameters used for different pellets

Elemental power	Compaction pressure (MPa)	Sintering temp (°C)	Holding time (h)	atmosphere
$Al_{70}Cu_{22}Ti_8$	450	900	2	argon
	450	1000	1	argon
	450	1100	1	argon
$Al_{70}Cu_{22}Ti_8$ - TiO_2 (1 wt. %)	450	900	2	argon
	450	1000	1	argon
	450	1100	1	argon
$Al_{70}Cu_{22}Ti_8$ - Y_2O_3 (1 wt. %)	450	900	2	argon
	450	1000	1	argon
	450	1100	1	argon

3.2 Characterization techniques used

3.2.1 X-Ray Diffraction (XRD) study

X-Ray diffraction (PAN analytical model: DY-1656) was used for determination of phases present in $(Al, Cu)_3Ti$ intermetallic compound. The polished pellets were mounted on sample holder of XRD machine and diffraction pattern was recorded with scanning range and step size of 30-100^0 and 3^0 / min respectively. The phase identification was done by 2θ value of the XRD pattern by using Cu K_α (λ=1.541^0) radiation. The experimental data was compared with that standard powder diffraction pattern using JCPDS.

3.2.2 Optical microscopy study

Optical microscopy is the primary tool for study of microstructure of any material. Leica DM microscopy with carl zeiss lens was used to primary investigate the surface morphology of $(Al,Cu)_3Ti$ intermetallic compound.

3.2.3 Scanning electron microscopy (SEM) study

Scanning electron microscopy (JEOL 6480 LV) was used for microstructural characterization of (Al, $Cu)_3Ti$ intermetallic powders. Micrographs were taken at 20KV of accelerating voltage. The microstructural study of intermetallic powders was observed from SEM micrographs. Electron dispersive spectroscopy (EDS) was used for compositional analysis of intermetallic powders.

3.2.4 Field Emission Scanning Electron Microscopy (FESEM) study

Filed emission scanning electron microscopy (Model: Nova Nano SEM450) was used for microstructural characterization of polished (Al, $Cu)_3Ti$ intermetallic pellets by FEITM made in Czech Republic, with electron dispersive spectroscopy (EDS) from BRUKER (liquid nitrogen free, made in Germany It carried a high resolution in vacuum mode is 1nm at 15kv with spot size 1 and magnification up to 6 lakhs. . Micrographs were taken at 5KV accelerating voltage. Its working principle is same as SEM, only the electron emission principle is different i.e. field emission. The morphological structure of intermetallic pellets was observed from FESEM micrographs. Electron dispersive X-Ray (EDX) was used for compositional analysis of intermetallic pellets.

3.2.5 Particle size measurement (PSM) study

Particle size of elemental power of $Al_{70}Cu_{22}Ti_8$ was measured by Malvern laser particle size analyser. PSM shows the variation in median size with milling time.

3.3 Physical properties study

3.3.1 Density measurement

Density of sample was calculated by common formula i.e. density is the mass of that material divided by volume. We calculated green density, sintered density, theoretical density and densification parameter. Weight of pellets measured by balanced machine after and before sintering and slide calliper was used for measuring the length and thickness of pellet before and after sintering. The density of sample calculated after sintering of the sample then it is called sintered density. The density of sample calculated before sintering take place called green density.

3.3.2 Differential scanning calorimeter (DSC) study

DSC was carried out by using NETZSCH DSC analyser by heating the powder from room temperature to 1000°C at the heating rate of 10°C under argon atmosphere. Here the sample is placed to a control temperature.

3.4 Mechanical properties study

3.4.1 Hardness measurement

Vickers hardness tester (Leco Micro-hardness Tester LM248AT) was used for measurement of hardness of the samples. The sample is policed by 0, 2, 3 ,4 emery paper by mechanically. Here the indentor we used is diamond. Most of the maximum sample prepared by power metallurgical route is given maximum load of 100gf force. A load of 50gf was applied for 10 seconds continuously. Minimum 7 measurements were taken at equivalent location for each sample to get consistent results.

3.4.2 Wear study

The wear test machine (Model no: DUCOM-TR-20-M100) was used for measurement of wear depth on the samples. The wear here is carried out is the pin on disk wear having dry sliding condition. The load of 20N given to the policed base alloy, TiO_2 and Y_2O_3 dispersed alloy and rotation given to the wear machine is 20rpm. The sliding time is 15min for each alloy and volume loss of the material also collected before each test.

Mathematically,

Wear volume(mm^3) = 2π x track radius x track volume x wear depth.
Wear rate ($mm^3\ N^{-1}\ m^{-1}$) = wear volume / (normal load × sliding distance).

3.4.3 Thermal conductivity study

Thermal conductivity of elemental power of $Al_{70}Cu_{30}Ti_8$ was measured by KD2 Pro DECAGON device. The probe is inserted to sample container and data will show on monitor of this device. Minimum 7 measurements were taken at equivalent location for each sample to get consistent results.

Fourier's law of conduction formula,

$$Q = -K\,A\,\frac{dT}{dx}$$

Where Q = Heat transfer

K=Thermal conductivity

A= Surface area perpendicular direction of heat transfer

$\frac{dT}{dx}$ = Temperature gradient

3.5 Flow Chart of experimental procedure

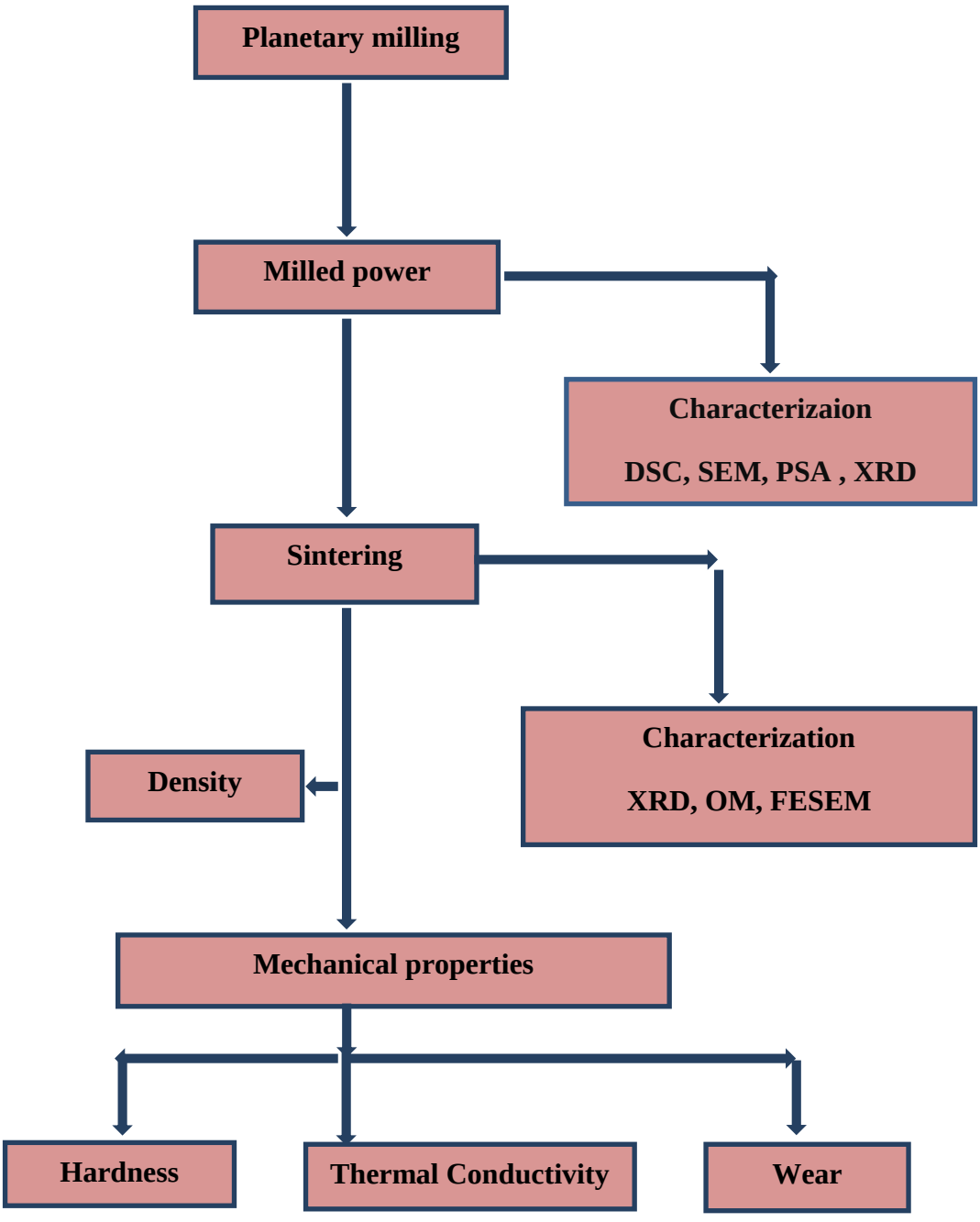

Figure 3.1 Flow chart of experiment

Chapter 4

Results and discussion

In this chapter synthesis and characterization of milled powder and consolidated intermetallics has been carried out. Physical properties like density and mechanical properties like hardness and wear have been studied.

4 Results and discussion

4.1 Synthesis of $(Al, Cu)_3Ti$ powder blend by mechanical alloying

4.1.1 X-ray diffraction (XRD) study of milled powder

Figure 4.1 shows the XRD spectra of $Al_{70}Cu_{22}Ti_8$ powder milled for different time periods. It has been observed from graph that intensity of pure elements like Al, Cu, Ti gradually decreases with milling. After 50h of milling, peaks of Cu_9Al_4, AlCu, $AlTi_3$ are visible. It is also seen that intensity of intermetallics increases gradually with milling. It has also been observed that XRD peaks became broaden during milling due to lattice strain and refinement of powders.

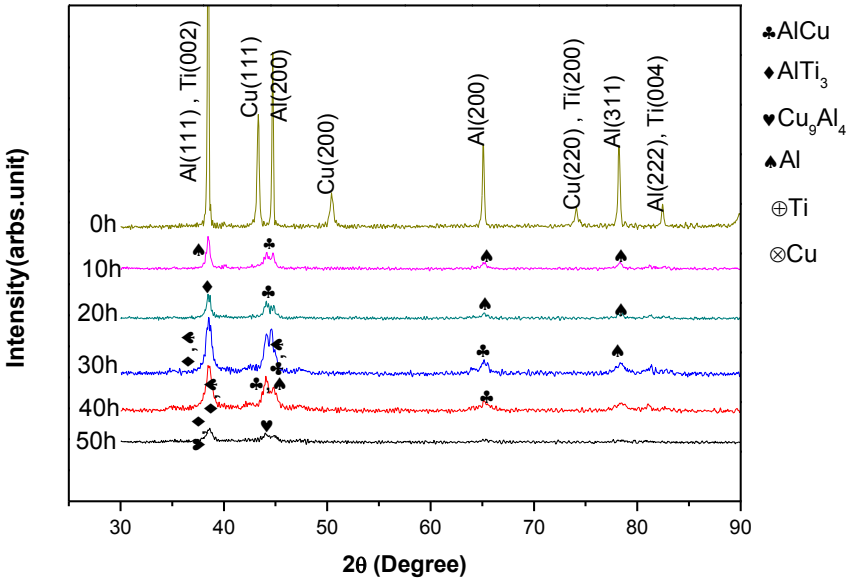

Figure 4.1 XRD spectrum of $Al_{70}Cu_{22}Ti_8$ intermetallic powder milled for different time periods

4.1.2 Particle size analysis

Figure 4.2 shows the particle size distribution of $Al_{70}Cu_{22}Ti_8$ powder milled for different time period. It has been observed that distribution graph shift to left side indicating reduction of particle size. It has been found that medium particle size reduces from 45 to 6 μm after 50 h of milling.

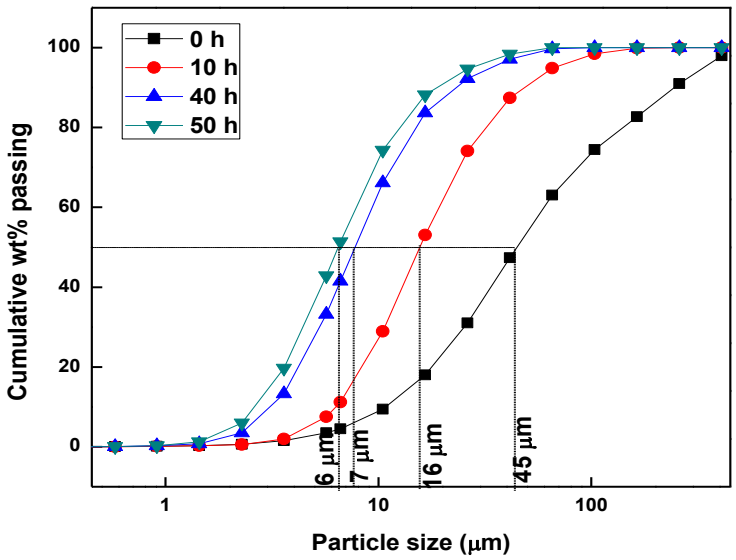

Figure 4.2 Particle size distribution of powder milled for different time.

Figure 4.3 shows the variation of median size with milling time. It has been observed from graph that the rate of reduction of size is very fast up to 10h of milling and after that it is gradually decreases and remains constant after 40 h of milling. During milling, both particle size reduction and agglomeration phenomena take place side by side. After 10 hours of milling an equilibrium has been reached.

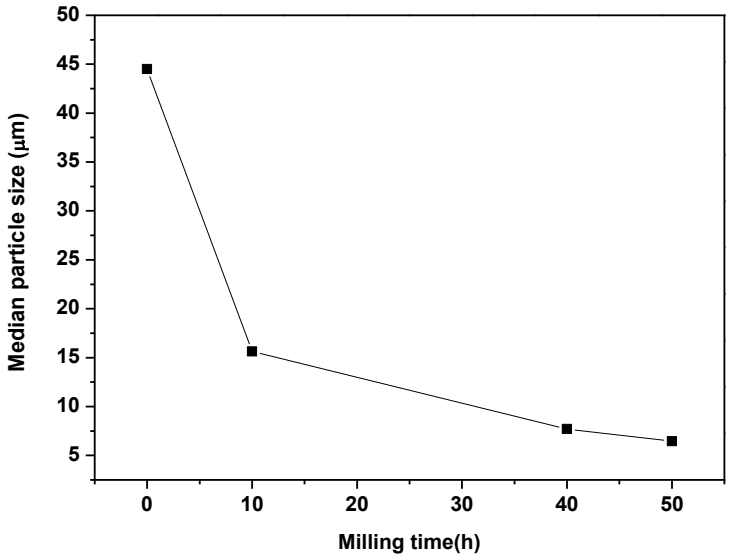

Figure 4.3 Variation of median size with milling time.

4.1.3 Differential Scanning Calorimeter (DSC) study

Figure 4.1.4 shows that the DSC graph of as mixed and 50h milled $Al_{70}Cu_{22}Ti_8$ powder. Both the powders were heat to 1000C at the heating rate of 10°C/min under Ar gas. From the graph it can been seen an endothermic peak at 660°C which represent the melting of aluminium in case of as mixed power. However, the peak is absent in case of milled power which represent pure aluminium is not present after 50 h of milling. Two exothermic peaks at 701 and 850°C are present due to the formation of intermetallics like $AlTi_3$, Cu_9Al_4 and AlCu and one endothermic peak at 535 is present due to the formation of Al_2Cu.

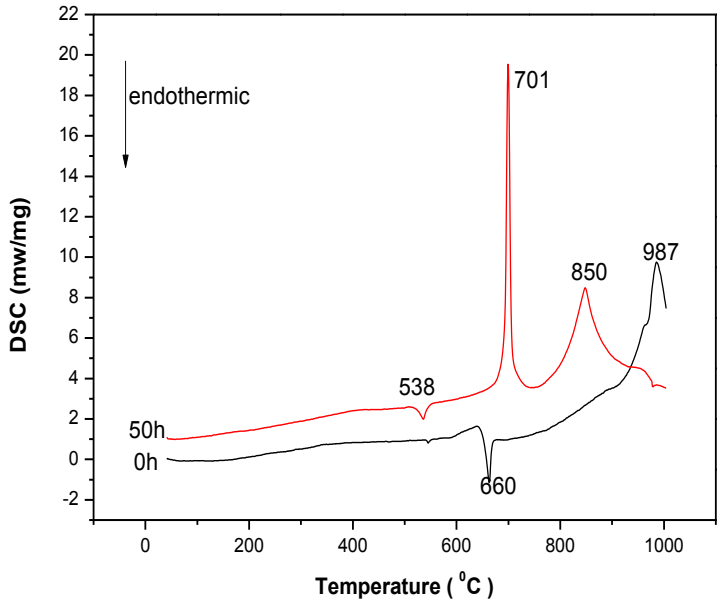

Figure 4.4 DSC plot of milled $Al_{70}Cu_{22}Ti_8$ powder subjected to heating up to 1000°C at the rate of 10^0C /min.

4.1.4 Scanning electron microscopy (SEM) study

Figure 4.5 shows the SEM micrographs of $Al_{70}Cu_{22}Ti_8$ powder milled for different time period. All the micrographs are taken at the magnification of 1000X. It is seen that the as received powder particle is large and bulky. Particle size gradually decreases as milling progresses. It can be seen that structure is relatively fine and homogeneous with increase in milling time. It can be found that after 0h milling particle size is around is 40 to 50 μm and after 30 h of milling the particle size is 10 to 20 μm. After 50 hours of milling particle size is around 5-10μm.

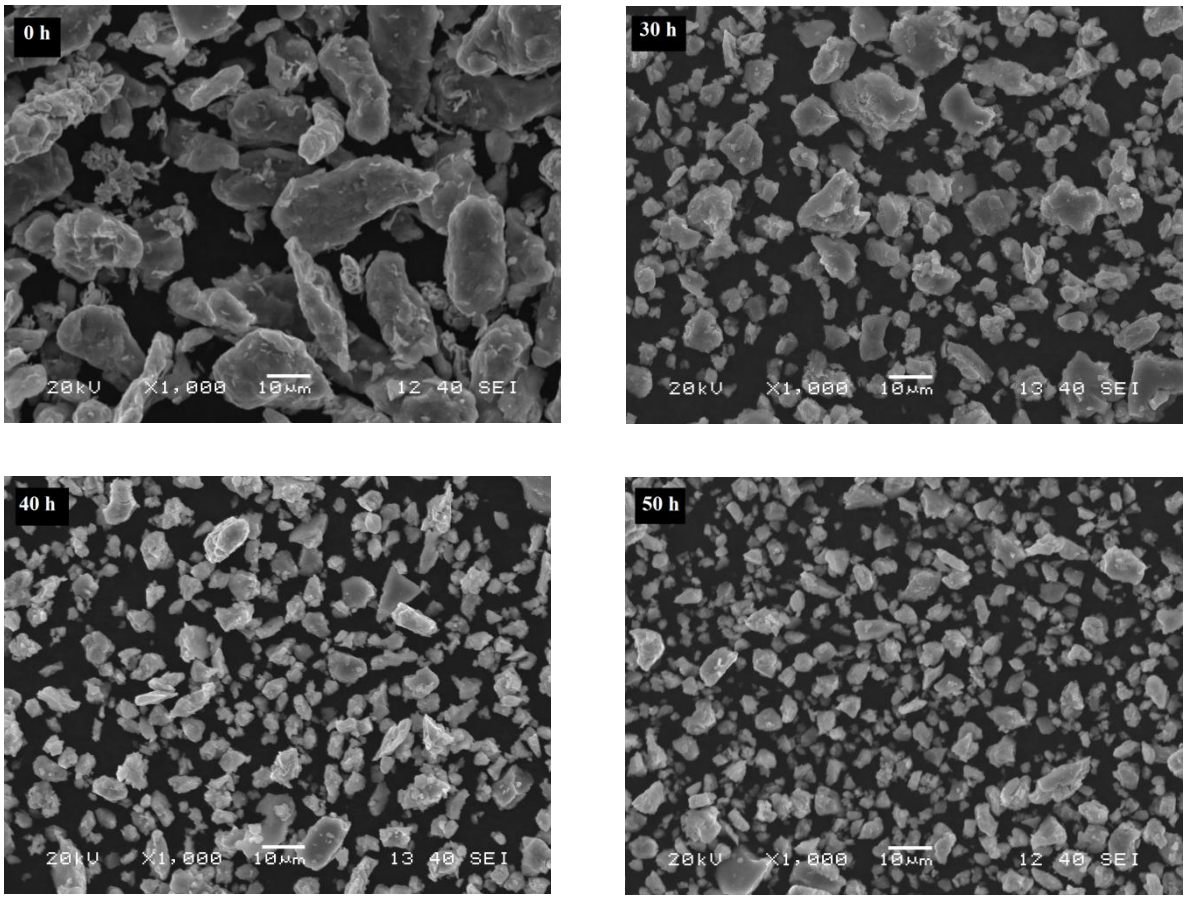

Figure 4.5 SEM micrographs of 0, 30, 40 and 50h milled powder.

Figure 4.6 shows the EDS spectrum and quantitative analysis of 50 h milled $Al_{70}Cu_{22}Ti_8$ milled. The spectrum was taken from whole micrograph of $Al_{70}Cu_{22}Ti_8$. The spectrum confirms the presence of aluminium, copper and titanium. The quantitative value of aluminium, copper and graphite are shown in table.

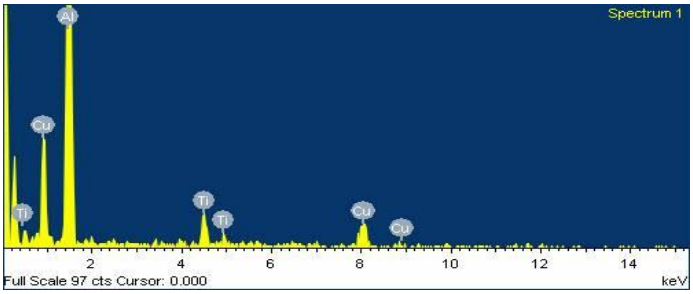

Element	Weight%
Al	69.32
Cu	22.63
Ti	8.05
Total	100

Figure 4.6 EDS spectrum and quantitative analysis of $Al_{70}Cu_{22}Ti_8$ powder milled for 50h

4.1.5 Thermal Conductivity

Table 4 shows the thermal conductivity of as mixed and 40h milled base powder $Al_{70}Cu_{22}Ti_8$. Experimentally we found the thermal conductivity of 0h and 40h milled powder are 0.039w/mK and 0.121 w/mK respectively at room temperature (35^0C). The thermal conductivity of 40 h milled powder is higher than as mixed powder as the grain size became small and mean free path of atoms become more and the availability of energy increases after milling.

Table 4 Thermal conductivity of base milled powder of composition $Al_{70}Cu_{22}Ti_8$

Milling Time	**Temperature (^{0}C)**	**Conductivity (w/mK)**
0h	35	0.039
40h	35	0.121

4.2 Consolidation of $(Al, Cu)_3Ti$ powder blend by conventional sintering

4.2.1 X-Ray Diffraction (XRD) study

Figure 4.7 shows the XRD spectra of 50h milled base powder $Al_{70}Cu_{22}Ti_8$ and TiO2 dispersed base powder sintered at 900^0C for 2h under argon atmosphere. It is found that there is a formation of Cu_9Al_4, Cu_3Ti and $CuAl_2$ intermetallics for the base composition after sintering. Formation of Al_2O_3 and Cu_3TiO_4 is evident from XRD spectrum due to reaction of TiO2 with base sample after sintering.

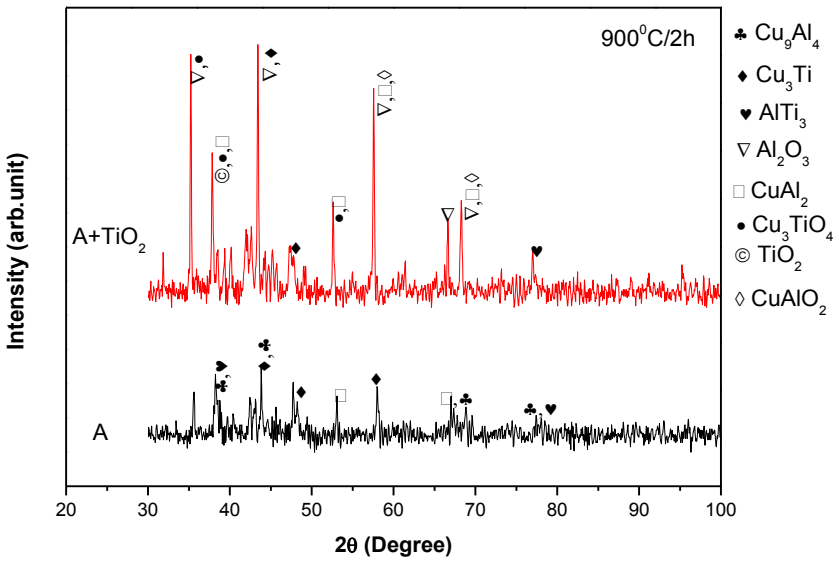

Figure 4.7 XRD spectrums of base powder of composition $Al_{70}Cu_{22}Ti_8$ and TiO_2 dispersed intermetallic at 900^0C for 2 h.

Figure 4.8 shows the XRD spectrum of 50h milled base powder $Al_{70}Cu_{22}Ti_8$, Y_2O_3 and TiO_2 dispersed base powder sintered at 1000 for 1h under argon atmosphere. It is found that the aluminium present in the base composition reacts with TiO_2 and Y_2O_3 separately and formation of Al_2O_3 takes place. In case of Y_2O_3 dispersed sample, there is a formation $Al_2Y_4O_9$ due to the reaction of Y_2O_3 with base composition.

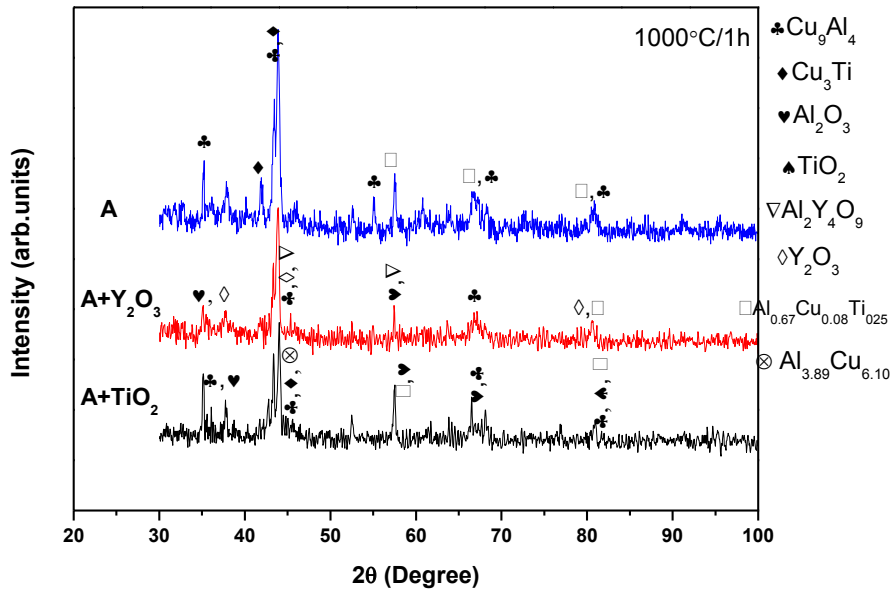

Figure 4.8 XRD spectrum of base power of composition $Al_{70}Cu_{22}Ti_8$ and Y_2O_3 ,TiO_2 dispersed intermetallic at 1000^0C for 1 h

Figure 4.9 shows that XRD spectra of 50h milled base power $Al_{70}Cu_{22}Ti_8$, TiO_2 dispersed base powder sintered at 1100 for 1h under argon atmosphere. In base sample the peaks of $AlCu_4$ and $CuAl_2$ peaks are visible. Here, aluminium reacts with Copper to form these above compounds. XRD spectra show the peaks of Al_2O_3, Cu_3TiO_5, $CuAlO_2$ and $CuTi_3$. Formation of these above compounds may be possible due to the reaction of TiO2 with Cu and Al.

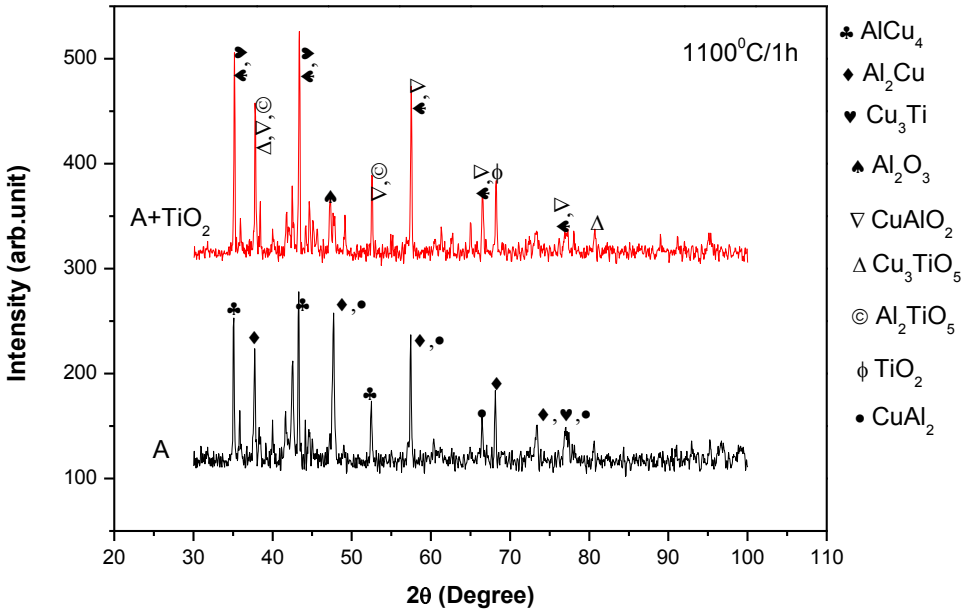

Figure 4.9 XRD spectrum of base power of composition $Al_{70}Cu_{22}Ti_8$ and Y_2O_3 ,TiO_2 dispersed intermetallic at 1100^0C for 1 h

4.2.2 Optical Microscopy (OM) Study

Figure 4.10 (a), (b) and (c) show the optical micrographs of the base powder $Al_{70}Cu_{22}Ti_8$, TiO2 dispersed and Y2O3 dispersed base powder sintered at 1000^0C for 1h under argon atmosphere. In present optical investigation, the micrograph depict that the grain structure is uniformly distributed everywhere and some areas have enlarge grains structure. It is evident from micrograph that the $Y2O_3$ and TiO_2 are dispersed uniformly with the base alloy.

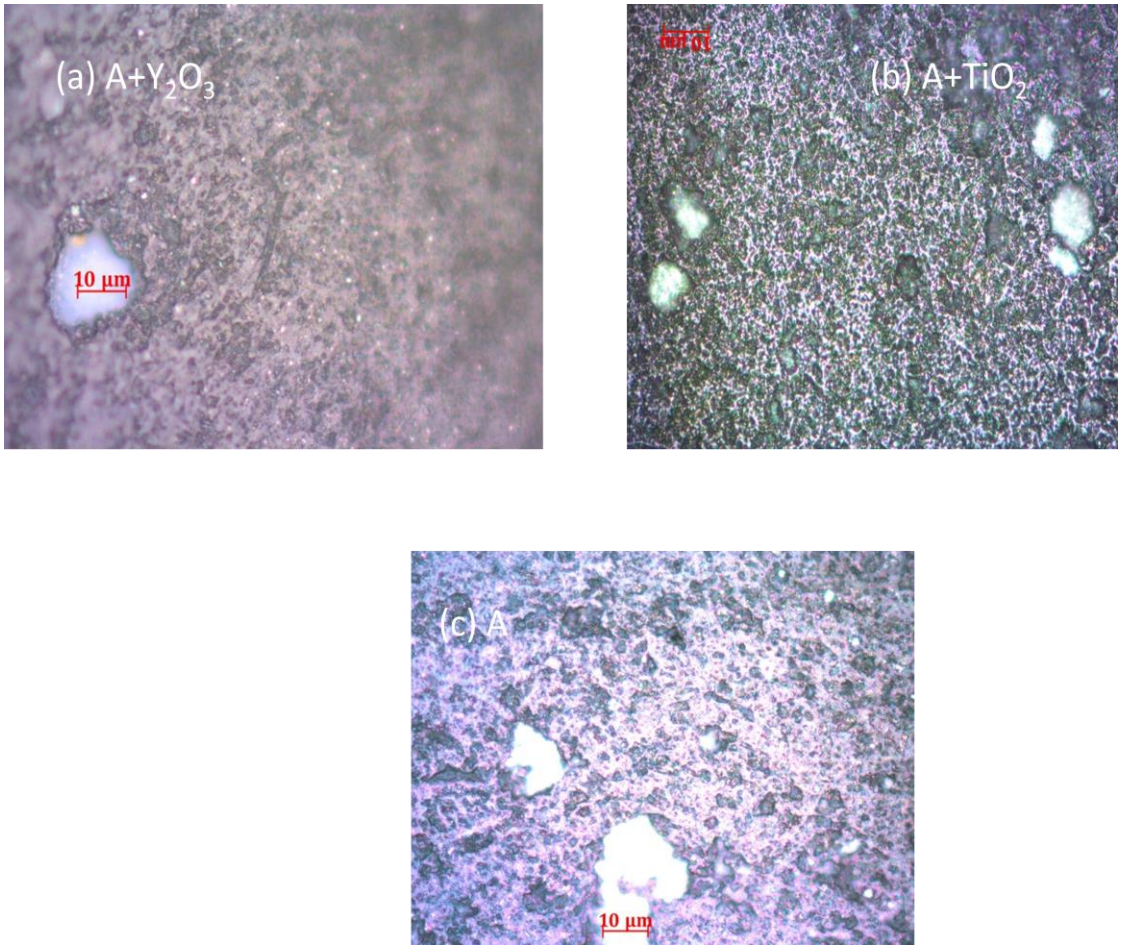

Figure 4.10 Optical micrographs of (a) Y_2O_3 dispersed base alloy (b) TiO_2 dispersed base alloy and (c) base alloy sintered at 1000°C for 1 h.

4.2.3 Field emission scanning electron microscopy (FESEM) study

Figure 4.11 (a) & (b) show the FESEM micrographs of base alloy and (c) & (d) show the FESEM micrographs of TiO_2 and Y_2O_3 dispersed base alloy sintered at 1000°C for 1 h under argon atmosphere. The micrographs reveal the presence of porosity in all the samples but it is less in Y_2O_3 and TiO_2 dispersed sintered samples as compared to base alloy. The different contrast in the micrographs shows the presence of various phases. The particle size after consolidation of nano Y_2O_3 and TiO_2 dispersed base alloys are shown in the micrographs. It is also seen that particle size drastically increases after consolidation at 1000°C for 1 h by conventional sintering.

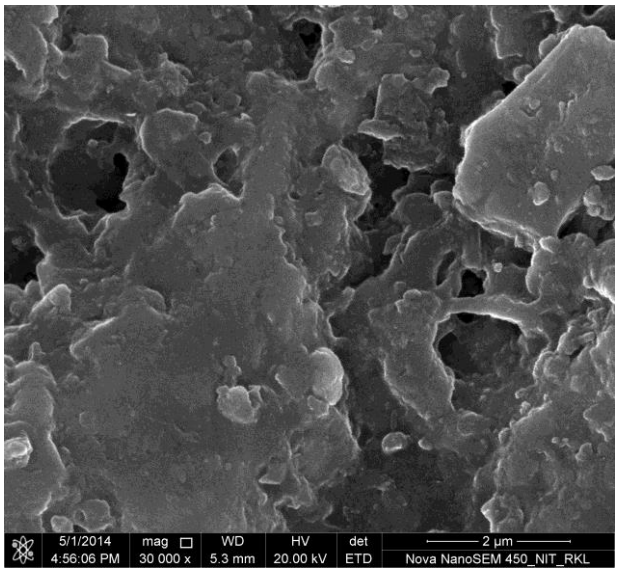

(a)

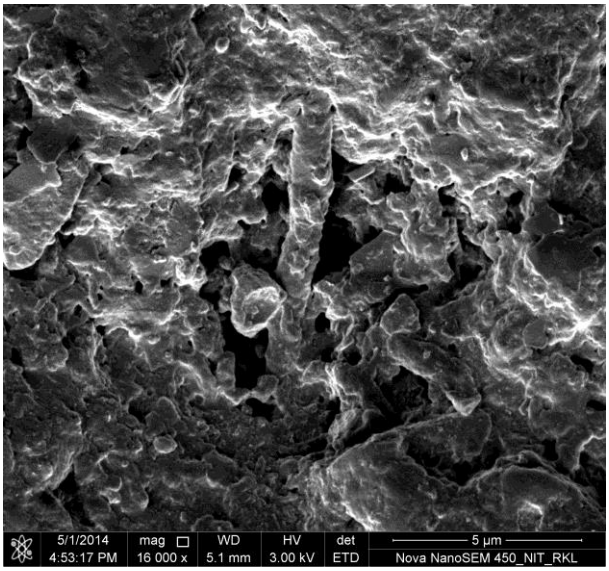

(b)

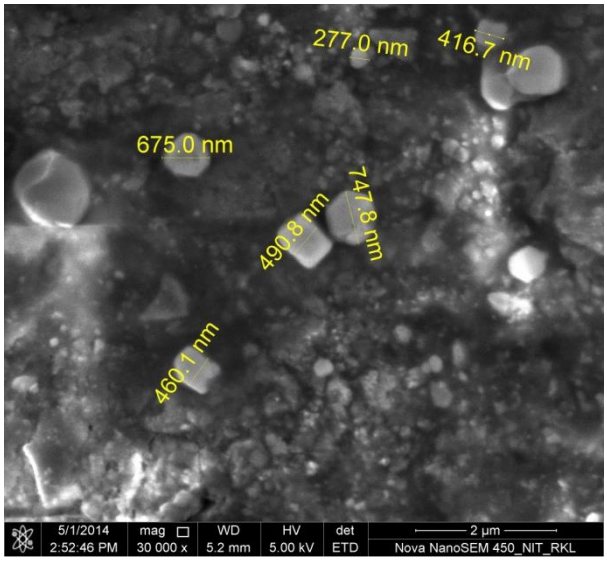

(c)

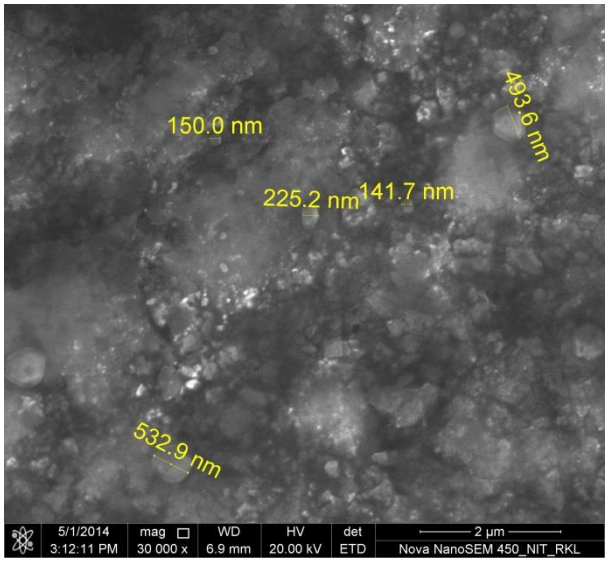

(d)

Figure 4.11 FESEM micrographs of (a) & (b) base alloy-A, (c) TiO_2 dispersed base alloy (d) Y_2O_3 dispersed base alloy sintered at 1000°C for 1 h.

4.2.4 Density Measurement

Figure 4.12 (a) shows the green density, sintered density and theoretical density of base alloy having sintered at 900, 1000 and 1100°C. It is observed from the graph that green density and theoretical density remain same for the same base alloy composition. The green density and theoretical density are 1.977gm/cc and 3.316gm/cc respectively. The graph depicts that as temperature increases the sintered density increases. As sintering temperature increases, rate of diffusion of atoms increases and eventually mass transfer takes place. As a result, the

particles are bonded together and neck formation takes place. Finally, porosity decreases and results in higher density with increasing temperature. The sintered densities are 2.171, 2.398 and 2.487gm/cc at 900, 1000 and 1100°C respectively.

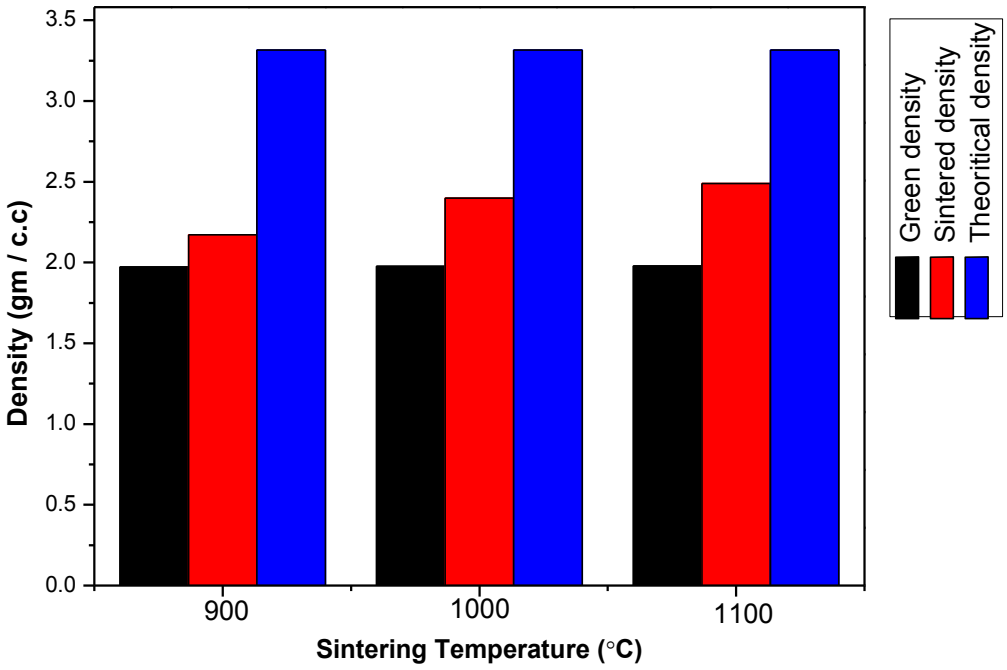

Figure 4.12 (a) Variation of green density, sintered density and theoretical density with sintering temperature for base alloy of composition $Al_{70}Cu_{22}Ti_8$

Figure 4.12 (b) and (c) shows the density of base alloy with TiO_2 and Y_2O_3 dispersed having sintered at 900 , 1000 and 1100^0C respectively. It is observed from the graph that green density and theoretical density remain same for the TiO_2 and Y_2O_3 composition. The green density and theoretical density of TiO_2 dispersed are 1.989gm/cc and 3.302gm/cc respectively and similarly the green density and theoretical density of Y_2O_3 dispersed are 1.927gm/cc and 3.306gm/cc respectively. The graph depicts that as temperature increases the sintered density increases. As sintering temperature increases, rate of diffusion of atoms increases and eventually mass transfer takes place. As a result, the particles are bonded together and neck formation takes place. Finally, porosity decreases and results in higher density with increasing temperature. The sintered densities are 2.246, 2.489 and 2.679gm/cc at 900, 1000 and 1100°C respectively for TiO_2dispersed and similar trend for Y_2O_3 dispersed the sintered densities are 2.235, 2.425, 2.635gm/cc respectively.

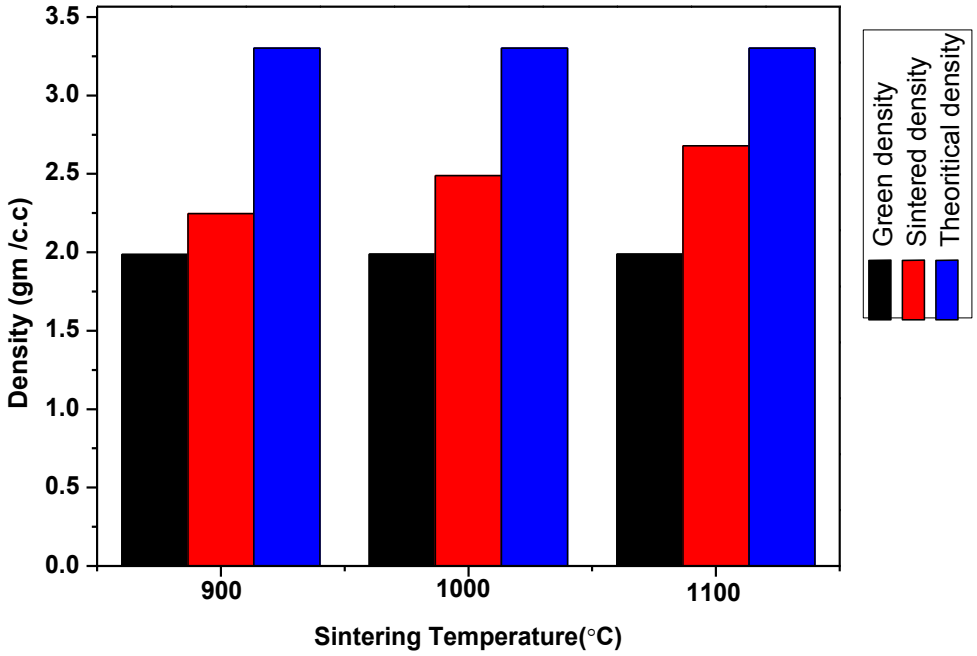

Figure 4.12 (b) Variation of green density, sintered density and theoretical density with sintering temperature of 1 wt. % TiO_2 dispersed base alloy

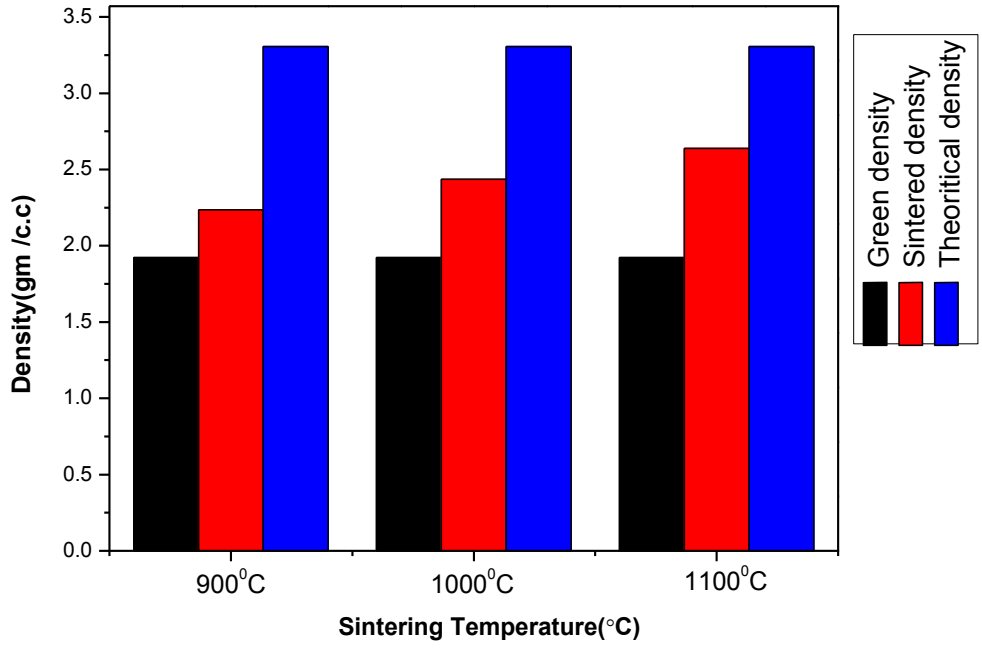

.

Figure 4.12 (c) Variation of green density, sintered density and theoretical density with sintering temperature of 1 wt. % Y_2O_3 dispersed base alloy

4.2.5 Densification parameter

Densification parameter (DP) is calculated by using the formula given below.

$$Densification\ parameter = \frac{Sintered\ density - Green\ density}{Theoretical\ density - Green\ density}$$

Figure 4.13 shows the variation of densification parameter of base alloy $Al_{70}Cu_{22}Ti_8$, TiO_2 dispersed base alloy and Y_2O_3 dispersed base alloy with sintering temperature. It is observed from the graph that densification parameter increases with temperature indicating higher rate of densification at higher temperature. The DP value for base alloy increases from 0.15 to 0.38 as temperature increases from 900 to 1100°C. The similar trend is followed for Y_2O_3 and TiO_2 dispersed base alloy. The increase in DP with temperature is due to higher rate of diffusion and results in higher shrinkage.

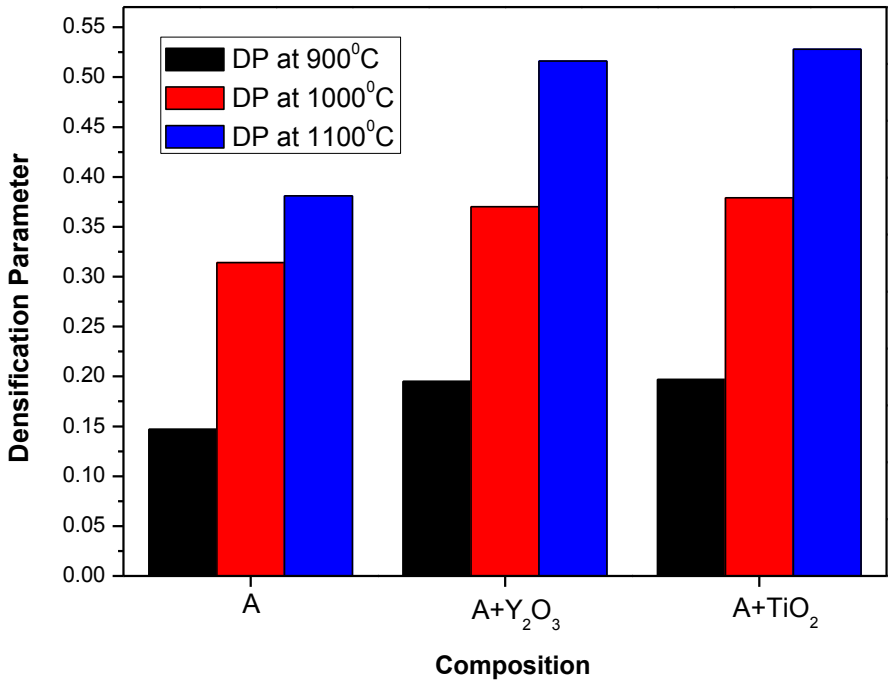

Figure 4.13 Variation of densification parameter of base alloy $Al_{70}Cu_{22}Ti_8$, TiO2 dispersed base alloy and Y_2O_3 dispersed base alloy with sintering temperature

4.2.6 Hardness measurement

Figure 4.14 shows the hardness of $Al_{70}Cu_{22}Ti_8$ (base alloy), Y_2O_3 and TiO_2 dispersed base alloy sintered at 900, 1000 and 1100°C respectively. It is shown from the graph that hardness of base alloy and Y_2O_3 and TiO_2 dispersed base alloys increases with temperature. However, the rate of increase of hardness of base alloy is less as compared to Y_2O_3 and TiO_2 dispersed base alloy. The hardness values of base alloy increases from 409 to 449 as sintering temperature increases from 900 to 1100°C. With the addition of 1 wt. % nanoY_2O_3 and TiO_2 hardness drastically increases. The hardness values of Y_2O_3 dispersed base alloy are 421, 442 and 649 at 900, 1000 and 1100°C respectively. Similarly, the hardness value of TiO_2 dispersed base alloy are 572, 593 and 872 at 900, 1000 and 1100°C respectively. From the hardness data it is clear that hardness is highest for TiO_2 dispersed alloy and lowest for base alloy. The hardness increases drastically with the addition of hard and brittle TiO_2 and Y_2O_3 particles. Another reason of high hardness after addition of TiO_2 and Y_2O_3 particles is due to the formation of hard and brittle Al_2O_3 phase as evident from XRD spectrum.

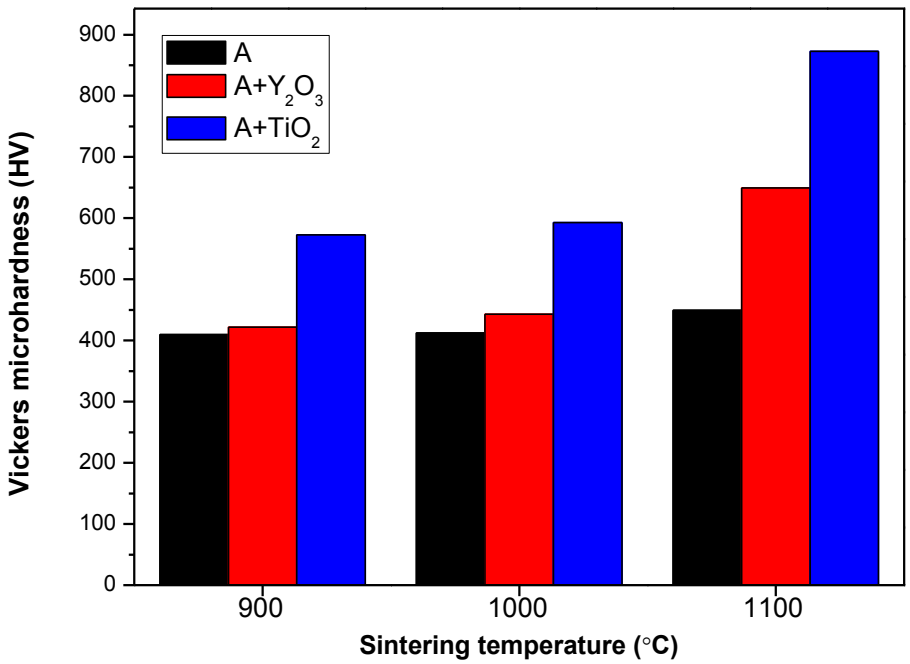

Figure 4.14 Bar chart of Vickers microhardness of $Al_{70}Cu_{22}Ti_8$ (base alloy), TiO_2 and Y_2O_3 dispersed base alloy sintered at different temperatures

4.2.7 Wear study

From 4.15 shows the variation of wear depth with sliding time of $Al_{70}Cu_{22}Ti_8$ (base alloy), Y_2O_3 and TiO_2 dispersed base alloy sintered at 1000 and 1100°C respectively. It is observed from both graphs that the wear depth decreases with the addition of Y_2O_3 and TiO_2 to the base alloy. The reason is that hard and brittle TiO_2 and Y_2O_3 spread all over the intermetallic uniformly and reduces the pores and providing strong interfacial bond. Watanabe et al. studied the wear behaviour of Al-Al_3Ti composite and showed that wear resistance is more for the composite as compared to pure Al. The abrasion is the main mechanism of wear on Al-Al_3Ti composite. The found that the supersaturated Al_3Ti layer formation occurs from the top surface to 100μm depth. It is seen from the graphs that samples sintered at 1100°C shows more wear resistance than 1000°C due to higher hardness. The maximum wear depth of base alloy sintered at 1100°C is around 200μm, whereas wear depth is 340μm for base alloy sintered at 1000°C. This is due to higher hardness at 1100°C as compared to 1000°C.

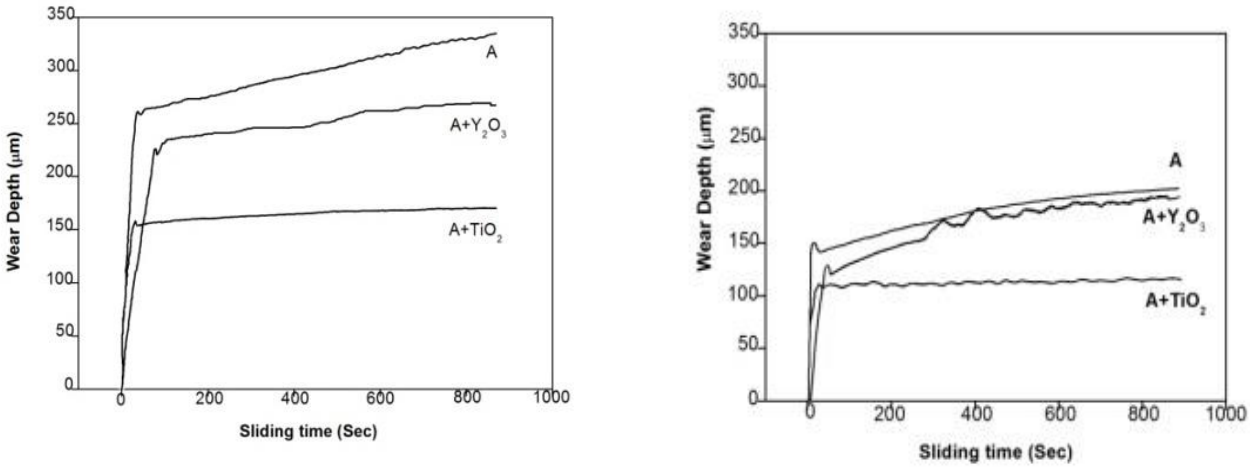

(a) (b)

Figure 4.15 (a) and (b) Variation of wear depth with sliding time of $Al_{70}Cu_{22}Ti_8$ (base alloy), Y_2O_3 and TiO_2 dispersed base alloy sintered at 1000 and 1100°C.

4.2.8 Weight loss during wear

Figure 4.16 depicts the weight loss during wear test of samples sintered at 1000°C for 1h.The graph shows that weight loss is lowest for TiO2 dispersed base alloy and highest for base alloy ($Al_{70}Cu_{22}Ti_8$). This is due to higher wear resistance of TiO_2 and Y_2O_3 dispersed base alloy as compared only base alloy.

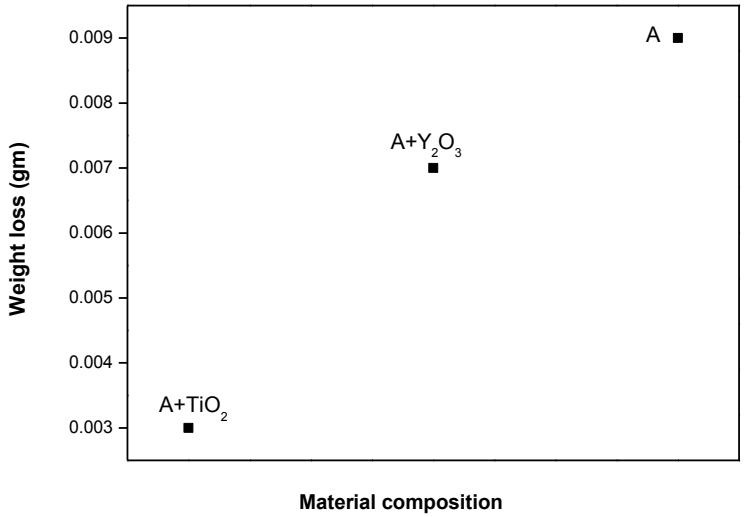

Figure 4.16 Weight loss during wear test of samples sintered at 1000°C for 1h

Chapter 6

Conclusions

Conclusions

The following conclusions can be drawn from the present investigation

1. The XRD study shows the peaks of Cu_2Al_4, AlCu, $AlTi_3$ intermetallics phases after 50 h of milling in case of base alloy. After consolidation of the base alloy, formation of new phases like Cu_9Al_4, Cu_3Ti, $CuAl_2$ are visible for the alloy sintered at 900 and 1000^0C but phases like Al_2Cu, $AlCu_4$ also visible for sintering at 1100^0C. After addition of TiO_2 and Y_2O_3 in base alloy there is formation of Al_2O_3.
2. Partcle size analysis confirms that as milling progresses the size of particle reduces and after 50h it is 6μm and SEM micrograph also confirm the shape is irregular and very small.
3. From DSC analysis we confirm that there is no melting endothermic peak of Al is present after 50h of milling and many exothermic peaks are obtained due to formation of intermetallic like $AlTi_3$, Cu_9Al_4 and AlCu.
4. The particle size after consolidation of nanoY_2O_3 and TiO_2 dispersed base alloys has been drastically increased after consolidation at 1000°C for 1 h by conventional sintering.
5. A maximum Vickers microhardness of 449, 649, 758HV were obtained for base alloy, Y_2O_3 and TiO_2 dispersed alloy sintered at 1100°C for 1h respectively. It was also found that TiO_2 and Y_2O_3 dispersed base alloy have higher wear resistance than base alloy.

Chapter 7

Future work

Future work

1. The effect of co-efficient of friction (μ) on wear behaviour to be investigated.
2. The electrical and magnetical properties of the $Al_{70}Cu_{22}Ti_8$, Y_2O_3 and TiO_2 dispersed sintered sample to be investigated.
3. The other advanced processing techniques such as spark plasma sintering, microwave sintering and hot isostatic pressing etc can be used for consolidation of $(Al, Cu)_3Ti$ intermetallic.
4. Other mechanical properties like roughness, fracture, transverse rapture strength can also be studied.

Chapter 8

References

References

[1] Schweitzer P.A.,"Metallic Materials, Physical, Mechanical and Corrosion Properties", CRC Press (2003)

[2] Callister W.D.,"Material Science and Engineering" 7th edition , John Wiley and Sons, University of Utah, (2007) pp. 577-578

[3] Sauthoff G.,"Intermetallic" , Chapman & Hall ,New york

[4] Mikkola D.E., Nic J.P., Zhang S., Milligan W.W., The Iron and Steel Institute of Japan international, 1991;31:1076

[5] Kumar K.S., Darolia R., Lewandowski J.J., Liu C.T., Martin P.L., Miracle D.B., Nathal M.V., editors," Structural intermetallics",Warrendale, USA: TMS; 1993. p. 87–96

[6] Varin R.A., Winnicka M.B., Virk I.S., In: Darolia R., Lewandowski J.J., Liu C.T., Martin P.L., Miracle D.B., Nathal M.V., editors. Structural intermetallics. Warrendale, USA: TMS; 1993. p. 117–24

[7] Shull R.D., Nanostruct Mater 1993;2:213

[8] Moon K.I., Chang K.Y., Lee K.S.J., Alloys Comp 2000;312:273

[9] Anton D.L., Duhn D.N., Giamci A.F.J, Miner Metals Mater Soc 1989;41:12

[10] Nayak S.S., Murty B.S.," Synthesis and stability of L12–Al3Ti by mechanical alloying" , Materials Science and Engineering A 367 (2004) 218–224

[11] Yamaguchi M.,Umakoshi Y.,Yamane T., Phil. Mag. 55 (1987) 301

[12] Kumar K.S.,Int. Mater. Rev. 35 (6) (1990) 293

[13] Yamaguchi M.,Umakoshi Y., Prog. Mater. Sci. 34 (1990) 1

[14] Baker I., Monroe P R., Met J.. 40 (1988) 28

[15] Mabuchi H., Hirukawa K., Tsuda H., Nakayama Y., Scripta Metall.24 (1990) 505

[16] Mazdiyasni S.,Miracle D.B.,Dimiduk D.M.,Mendiratta M.G.,Subramanian P.R.,Scripta Metall. 23 (1989) 327

[17] Mabuchi H., Hirukawa K., Nakayama Y.,Scripta Metall. 23 (1989)1761

[18] Suryanarayana C.,"Mechanical alloying and milling",Progress in Materials Science, 2001, 46, 1-184

[19] Nayak S.S.,Pabi S.K.,Murty B.S.,"Al–(L12)Al3Ti nanocomposites prepared by mechanical alloying: Synthesis and mechanical properties" Journal of Alloys and Compounds 492 (2010) 128–133

[20] Suryanarayana C.,Ivanov E., and Boldyrev V.V., "The science and technology of mechanical alloying" , Materials Science and Engineering, 2001, A304–306,151–158

[21] Soni P.R., "Mechanical alloying fundamentals and application" ,Cambridge, 2001

[22] Upadhyaya G.S.," Power metallurgical route", Cambridge, England, 2002

[23] Srinivasan S.,Chen S.R., Schwarz R.B, "Synthesis of A1/A13Ti two-phase alloys by mechanical alloying" Materials Science and Engineering, A 153 (1992) 691-695

[24] Watanabe Y.,Yamanaka N.,Fukui Y. "Wear Behavior of Al-Al_3Ti Composite Manufactured by a Centrifugal Method" , Metallurgical and materials transactions a volume 30a,december 1999—3261

[25] Milman Y.V.,Miracle D.B., Chugunova S.I., Voskoboinik I.V., Korzhova N.P., Legkaya T.N., Podrezov Y.N., "Mechanical behaviour of Al3Ti intermetallic and L12 phases on its basis" Intermetallics 9 (2001) 839–845

[26] Lee S.H., Moon K., Lee K.S., "Enhancement of the fracture toughness of bulk L12-based (AlC12.5 at. % M)3Zr (M Z Cu, Mn) intermetallics synthesized by mechanical alloying" Intermetallics 14 (2006) 1–8

[27] Nayak S.S., Pabi P.B., Murty B.S., "High strength nanocrystalline L12-Al3(Ti, Zr) intermetallic synthesized by mechanical alloying" Intermetallics 15 (2007)

[28] Wang S R., Li C., Yong W., Hou X., Geng H., Xu F., "Formation of La-modified L12–Al3Ti by mechanical alloying and annealing" Materials characterization 59 (2008) 44 0 – 446

[29] Fu Y., Shi R., Zhang J., Sun J., Hu G., "Microstructure and mechanical behavior of a multiphase Al3Ti-based intermetallic alloy" Intermetallics 8 (2000) 1251-1256

[30] Heilmaier M., Saage H., Eckert J.,"Formation of ODS L12–(Al, Cr)3Ti by mechanical alloying" Materials Science and Engineering A239–240 (1997)652–657